



New analysis and correlation between steady and oscillatory tests in fumed silica-based shear thickening fluids

Andres G. Moron¹ · Maria Jesus L. Boada¹ · Beatriz L. Boada¹ · Vicente Diaz¹

Received: 24 October 2018 / Revised: 25 March 2019 / Accepted: 2 July 2019 / Published online: 10 August 2019
© Springer-Verlag GmbH Germany, part of Springer Nature 2019

Abstract

In recent years, the non-Newtonian behavior of shear thickening fluids (STFs) has motivated a sharp increase in the number of studies related to their use for engineering applications. For this reason, rheological characterization of STFs is crucial in order to develop and design new devices based on these novel smart fluids. Typically, different experiments have been carried out for the rheological characterization of STFs to prove their shear/strain thickening behavior. In order to find an empirical relationship between steady and oscillatory experiments, the modified Cox-Merz rule has been recently used to correlate the results with enormous controversy between authors due to the disparity in the correlations achieved. In this paper, we present an improvement in the correlation between the results obtained in steady and oscillatory tests in STFs using fumed silica-concentrated suspensions. The proposed method with the use of strain sweep oscillatory tests has improved the correlation in all STF regimes (pre-transition, transition, and post-transition) in comparison with the results obtained using the modified Cox-Merz rule, which uses oscillatory frequency sweep tests. This improvement has been experimentally validated using concentrated colloidal suspensions with different concentrations of fumed silica (from 12.5 to 25 wt%).

Keywords Material modeling · Fumed silica suspension · Shear thickening · Modified Cox-Merz rule

Introduction

Recently, shear thickening fluids (STFs) have received increasing interest due to their unique characteristics as non-Newtonian fluids (Brown et al. 2010): (1) stress sharply jumps with raising shear rate, producing a solid-like behavior and (2) the reversibility of the thickening effect when the shear excitation is removed. These properties are one of the reasons why STFs are potential candidates for use in commercial applications such as liquid body armor due to their ability to absorb high amounts of energy on impact by projectiles at high velocity (Majumdar et al. 2014; Laha and Majumdar 2016; Li et al. 2016). In addition, the use of STFs is being researched in other fields such as in smart structures (shock transmission units or adaptive damping systems) and also transportation (vehicle viscous

dampers, rotational brakes, or speed bumps) (Ding et al. 2013; Zhang et al. 2008; Tian and Nakano 2017). Currently, shock transmission units (STUs) are being designed to be connected between structural members to form a rigid link under rapidly applied loads, while allowing the structure to move freely under slowly applied loads. These devices are frequently used to withstand the effects of earthquakes on structures. Taking into account how an STU filled with STF works, authors are researching in new industrial applications of this type of device such as the improvement of bus and coach structures (Galvez et al. 2017) installing these devices in order to absorb energy (Galindo-Rosales 2016) in the case of rollover. Rollover is one of the types of accidents where researchers have focused due to the gravity of injuries and the social impact it generates (Park and Yoo 2008; Liang and Le 2009; Gauchía et al. 2011). In consequence, for a correct design of this type of device, it is necessary to study in detail not only the geometrical parameters of the STUs but also how the properties of the STFs influence in the behavior of STUs.

The behavior of shear thickening-concentrated suspensions at low shear rates is known as Newtonian or slight shear thinning. Once a critical shear rate ($\dot{\gamma}_c$) is reached, the shear thickening transition takes place and a sharp increase of the viscosity occurs until the viscosity takes its

✉ Andres G. Moron
100081833@alumnos.uc3m.es

Maria Jesus L. Boada
mjboada@ing.uc3m.es

¹ Mechanical Engineering Department, Universidad Carlos III de Madrid, Avenida de la Universidad, 30 Leganés, Madrid, Spain

largest value (η_m), where the transition is finished (Galindo-Rosales et al. 2011a, b). Subsequently, beyond the shear transition point ($\dot{\gamma}_m$), different phenomenon may occur: fracture of the specimen due to the high viscosity, stabilization of the value of the viscosity independent of shear rate, or decrease of the viscosity with increasing shear rates (Fischer et al. 2007). This last phenomenon is observed in most cases of concentrated suspensions of fumed silica in organic polar liquids (Galindo-Rosales et al. 2009; Tian et al. 2015).

Although there is now a huge interest in the study of STFs, the mechanisms of the dramatic phenomenon of shear thickening in colloidal suspensions were not manifestly distinguished until recently. The order-disorder transition mechanism was first suggested by Hoffman (1972, 1974). Hoffman proposed that hexagonally packed layers of particles appear before the shear thickening transition. At low shear rates, these ordered layers form and move across each other, reaching the shear thinning region. However, at high shear rates, instability is produced where the repulsive forces between particles are overcome, resulting in a jump in viscosity value. Nevertheless, it has been proven that a shear thickening transition is able to arise without an order-disorder mechanism (Maranzano and Wagner 2002; Egres and Wagner 2005; Egres et al. 2006; Brown and Jaeger 2014). On the other hand, another theory which has been achieved to analyze shear thickening behavior is hydrocluster theory. The hydrocluster mechanism was first introduced by Bossis and Brady (1989).

The hydrocluster theory suggests that at a zero shear rate, in an equilibrium state, the structure of STFs is only affected by electrostatic and Brownian motion. However, at low and increasing shear rates, the contribution of Brownian force disappears and interparticle hydrodynamic forces leave. Despite the hydrodynamic forces, the streamlining caused by the formation of organized layers of particles parallel to the flow motion produces a decrease in the viscosity due to the ease of movement. When the stress is increased, at the onset of shear thickening, hydrodynamic instabilities are caused due to hydrodynamic interaction between particles that dominate over stochastic forces, and hydroclusters arise. The higher rates of energy dissipation and the sudden rise in viscosity are because of the impediment of particles flowing around each other (Bender and Wagner 1996; Wagner and Brady 2009). A greater increase of the viscosity is due to the formation of large clusters (Egres et al. 2006). Different techniques have confirmed hydrocluster theory in the shear thickening regime (Cheng et al. 2011; Lee and Wagner 2006).

While the hydrocluster mechanism has become an accepted theory for continuous shear thickening, it does not explain the enormous increase in viscosity occurring in discontinuous shear thickening (Brown et al. 2010). In this case, Brown and Jaeger (2012) has proposed

that it is the result of dilation of the particle packing during the onset of shear thickening. Other mechanisms for specific suspensions that complement the hydrocluster theory have been also proposed (He et al. 2015). In the last few years, the established view that shear thickening is caused by hydroclusters has been rejected due to recent simulations suggesting that contact forces dominate both in discontinuous and continuous shear thickening (Seto et al. 2013; Mari et al. 2014; Lin et al. 2015). The formation of multiple bands due to a discontinuity in the viscosity is other proposed mechanism in the last years (Vázquez-Quesada et al. 2017; Turcio et al. 2018). According to the complicated mechanism of shear thickening fluids, models which can predict different rheological phenomena are being studied (Manero et al. 2007; Garcia-Rojas et al. 2009). The use of these models could give a final answer about the mechanics of the thickening behavior with valuable contributions in the mechanical and thermodynamic instabilities, i.e., flow-induced phase transitions or shear banding instabilities.

The principal parameters which are significant with respect to the shear thickening phenomenon were described by Barnes (1989) in his influential review. Some of these parameters include the solid volume fraction, particle size and shape, particle size distribution, and particle interactions (Zhang et al. 2010). Nevertheless, one of the factors that has shown the greatest influence on shear thickening behavior in suspensions is the volume fraction (Hoffman 1972; Barnes 1989). When the particle concentration increases, it produces an increasing probability that these particles affect the flow field of others so hydrodynamic interactions are produced. These hydrodynamic interactions, at high volume fractions, have a considerable influence on the flow behavior (Mewis and Wagner 2012; Zhang et al. 2014). Recently, investigations have also been presented where the addition of additive particles is used to modify the characteristics of STFs (Gürgen et al. 2016; Gürgen et al. 2016). This knowledge about parameters and factors affecting shear thickening phenomenon is crucial for modifying and controlling the thickening stage, and therefore to be able to use STFs in engineering applications. Typically, both steady and oscillatory shear experiments have been carried out for the rheological characterization of STFs to prove their shear/strain thickening behavior. Furthermore, the modified Cox-Merz rule (also known as the Delaware-Rutgers rule) has been used to correlate the results between steady and oscillatory experiments with enormous controversy between authors due to the disparity in the correlations achieved (Zhang et al. 2008; Fischer et al. 2007; Chang et al. 2011; Nguyen et al. 2013; Lee and Wagner 2003).

The novelty of this work is to present a new analysis and correlation between steady and oscillatory tests of fumed silica-concentrated suspensions in a polar organic liquid

(polypropylene glycol). Steady and oscillatory shear tests have been performed under different particle concentrations to characterize the rheological behavior of the STFs proposed. On the one hand, in steady shear rheology, the response of the STFs is measured in terms of viscosity under an applied shear stress. Furthermore, the effects of fumed silica concentration on the most important parameters of the steady shear tests are studied to obtain the relationship between weight fractions, viscosities, and shear stress. On the other hand, in oscillatory shear rheology, both oscillatory frequency and strain sweep tests have been applied to the samples and the response of the STFs is analyzed in terms of two important viscoelastic parameters: elastic modulus (G') and viscous modulus (G''); moreover, oscillatory shear tests are also used to find a correlation with steady shear test. The validity of this correlation is discussed and compared with results obtained by other authors.

Materials and methods

Materials and sample preparation

The STF components used in this research were based on hydrophilic fumed silica SiO₂ (type S5130), with a primary spherical particle average size of 7 nm and a specific surface area BET of $395 \pm 25 \text{ m}^2 \cdot \text{g}^{-1}$. The carrier fluid was polypropylene glycol (PPG) C₃H₈O₂ (type 81370), with a molecular weight of $1200 \text{ g} \cdot \text{mol}^{-1}$. The viscosity and density of PPG 1200 at 20 °C were 270 mPa·s and $1.00 \text{ g} \cdot \text{ml}^{-1}$, respectively. Both materials were obtained from the Sigma Aldrich Corporation and all these properties were given based on the manufacturer's specifications.

In order to investigate the influence of fumed silica weight fraction on the dilatant effect of shear thickening fluid, different samples of STFs were studied. All samples were made in batches of 60 cm³. In each sample, 20 cm³ of PPG 1200 was mixed with the corresponding quantity of fumed silica for each weight fraction sample (from 12.5 to 25 wt%), as suggested in previous studies (Zhang et al. 2008; Tian and Nakano 2017; Tian et al. 2015; Gürgen et al. 2016). In each STF sample, certain amounts of fumed silica were dispersed in the carrier fluid in small increments (approximately 2.5%) until the final ratios of weight fraction were reached. The range of concentrations was selected from the percentage where the shear thickening effect was considerable to the percentage where critical packing fraction was reached. Suspensions were prepared by mixing at room temperature for 20 min using a blender (Bisen IQ250 equipped with spiral blades) at a velocity of 850 rpm. Once the samples were mixed, the batches were placed in a vacuum chamber for 0.5 h in order to remove any air bubbles which could have remained in the suspension

samples. Eventually, the samples were left at rest for least for 24 h before any measurements were obtained.

Experimental measurement methods

Rheological measurements were performed on a stress-controlled rheometer (AR 2000EX rheometer, TA Instruments) with a stainless steel parallel plate measuring system (25-mm plate diameter). Steady-state strain rate ramps and oscillatory frequency/strain sweeps were both carried out for each sample. In both steady and oscillatory tests, a gap size of 800 μm was used and the temperature was set at $30 \pm 0.1 \text{ }^\circ\text{C}$. Peltier temperature control was employed to fix the desired temperature. The pre-shear and rest protocols were defined following the recommendations provided by authors who used the same type of STFs (Galindo-Rosales et al. 2011a, b). This methodology has been already used in other works (Khandavalli and Rothstein 2014, 2015). Taking this into account, the rheometer was programmed to execute steady pre-shear at 1 s^{-1} for a 60 s duration in order to remove loading effects and once it had finished; a resting time period of 120 s was used to achieve an equilibrium structure. This procedure was carried out before each measurement. The steady shear tests were conducted by stress sweeps by varying shear stress from 1 Pa to the necessary value to achieve a post-transition regime in each sample. Each point of the plot was obtained after shearing the sample at a certain shear stress until the equilibrium was achieved. On the other hand, the oscillatory tests were performed by a strain sweep (from 10 to 2000%) at different constant frequencies and by a frequency sweep (from 1 to 100 rad·s⁻¹) at different constant strains. In oscillatory tests, each point was measured after two conditioning cycles and obtained from four sampling cycles. These values were determined in previous tests in order to ensure steady-state measurements. All rheological measurements presented in this work are reproducible.

Results and discussion

Rheological behavior of steady shear experiments

Figure 1 shows the shear rate dependence of viscosity for suspensions with different particle concentrations (from 12.5 to 25 wt%) by increments of 2.5 wt%. We found problems related with shear banding at high shear rate values (after shear thickening state). This effect produced macroscopic loss of material and wall slip. We decided to not have into account all data produced after shear banding, which is the reason why post-transition is only represented by few data points. Problems with the characterization of the post-transition behavior have been reported before

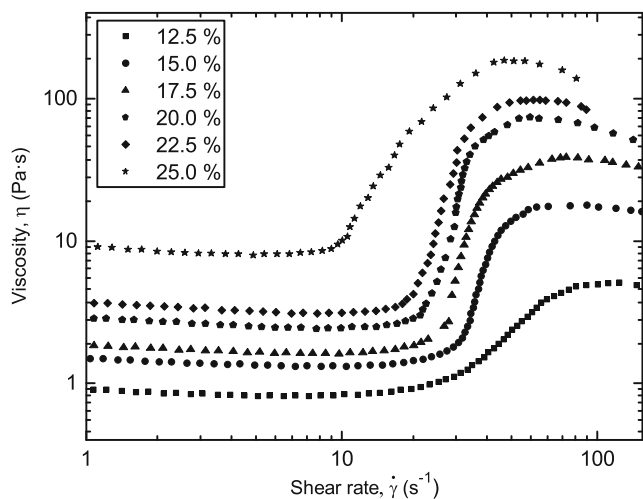


Fig. 1 Steady shear viscosity as a function of shear rate of different shear thickening fluid (STF) samples with fumed silica concentrations from 12.5 to 25 wt%

(Fischer et al. 2007; Egres and Wagner 2005; Lee and Wagner 2006) and those who provided post-transition data discussed the possibility of shear thinning behavior after the shear thickening regime was reached (Galindo-Rosales et al. 2011a; Seto et al. 2013). Shear thickening behavior is evident for all concentrations and occurs between two shear thinning regions; the first one is a weak shear thinning region for low shear rates and the second occurs at high shear rates once the maximum viscosity has been reached (Galindo-Rosales et al. 2009, 2011a, b). In the post-transition results that could be measured, it was observed that in high concentrations of fumed silica, where the maximum viscosity is much higher, the viscosity-decreasing slope in the stiffened regime was more abrupt than at low concentrations.

Figure 2 shows the data in Fig. 1 rescaled to investigate the most important parameters of the characterization of STFs. Critical and maximum shear stress as functions of fumed silica particle concentration are illustrated in Fig. 2a. The critical stress values were determined at the onset of the shear thickening regime and maximum stress values at the end. These values were obtained analyzing the evolution of slopes of the viscosity as a function of shear rate. The dependence of maximum shear stress on particle concentration can be seen, where increasing values of maximum shear stress are reached with increasing weight fraction. However, critical shear stress values show that shear thickening fluids appear at almost constant shear stress. These results are consistent with the concept that shear thickening is a stress-controlled phenomenon

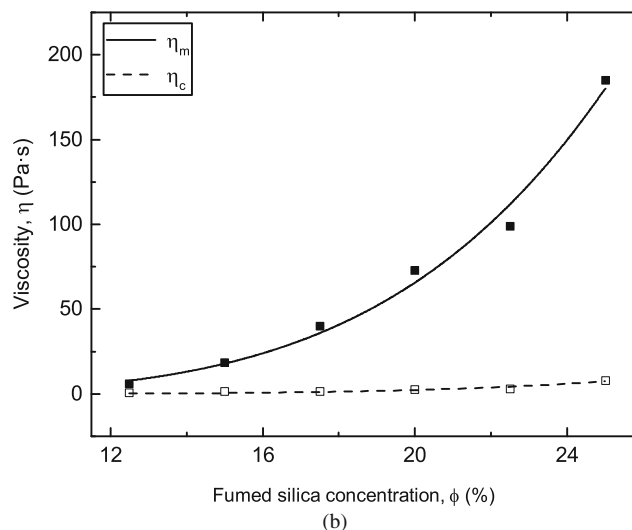
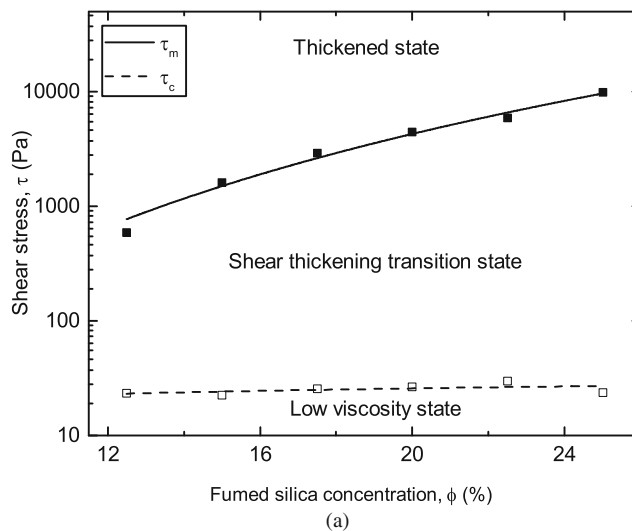


Fig. 2 **a** Critical shear stress (τ_c) and maximum shear stress (τ_m). **b** Critical viscosity (η_c) and maximum viscosity (η_m) as a function of weight fraction of fumed silica in the STF suspension. The lines show the best fit to power law

(Fischer et al. 2007; Bender and Wagner 1996; Mewis and Wagner 2012). In the figure, the pre-transition (low viscosity state), transition (shear thickening state), and post-transition (thickened state) phases are also represented and could be used to predict shear stress values with respect to the STFs' change of state as a function of fumed silica concentration. We examine the effect of particle concentration on critical and maximum viscosity in Fig. 2b. It can be noted, as expected, that the maximum viscosity of the STFs dramatically increases with increasing particle concentration. In addition, an increase in the critical viscosity occurs, but it is much less pronounced than that

experienced with increasing particle concentration in the maximum viscosity values.

Rheological behavior of oscillatory shear experiments

Oscillatory experiments were conducted to study the rheological properties of the STF samples. The viscoelastic response of the different fumed silica concentrations is illustrated in Fig. 3 in terms of strain sweep at a fixed angular frequency of $15 \text{ rad}\cdot\text{s}^{-1}$. It can be seen from this figure, for all concentrations, that both the elastic modulus (Fig. 3a) and viscous modulus (Fig. 3b) in the linear viscoelastic regime show a behavior where the elastic and viscous moduli are independent of the applied strain with G'' dominating over G' . At a certain critical strain amplitude, both moduli G' and G'' undergo an abrupt

jump transition to higher levels, exhibiting strain thickening behavior at a high strain amplitude. This phenomenon was explained as flow-blocking (reported in the previous work Zhang et al. 2014) which indicates that the STF materials exhibit both variable stiffness and damping capabilities (Zhang et al. 2008). These results are consistent with the hydroclustering theory and the previous results of nonfloculated suspensions (Raghavan and Khan 1997; Galindo-Rosales et al. 2009).

Figure 3 also shows that, for strain sweep tests, the transition to strain thickening behavior occurs in smaller strains as fumed silica concentration is increased in both elastic (Fig. 3a) and viscous moduli (Fig. 3b). This behavior is explained by the formation of larger clusters as the particle concentration is increased, and the presence of more clusters address to difficulties of particles flowing around each other. Therefore, the onset of strain thickening decreased when the concentration is increased. Furthermore, we have noted that for each concentration that the maximum elastic moduli are reached at smaller strains than the maximum viscous moduli. This means that when viscous moduli are still in the strain thickening transition regime, elastic moduli are already in the post-transition regime. These behaviors not only have been observed for strain sweep at $15 \text{ rad}\cdot\text{s}^{-1}$ but for all frequencies studied in this investigation. After finishing the strain thickening transition, it produced the strain thickening regime. This effect is similar to the behavior observed from steady shear tests.

The Cox-Merz rule is an empirical relationship that relates the linear viscoelastic behavior under steady and oscillatory shear. This rule has been satisfactorily used in polymer systems and dispersions, but it is not reliable for complex systems which present high nonlinearities. Doraiswamy et al. (1991) proposed a correlation between complex viscosities obtained from frequency sweep tests at fixed strain amplitudes and steady shear viscosities for suspensions with yield stress. This correlation is known as the modified Cox-Merz rule or the Delaware-Rutgers rule:

$$\eta^*(\gamma_0 \cdot \omega) = \eta(\dot{\gamma}) \quad (1)$$

Raghavan and Khan (1997) were the first to demonstrate the validity of this rule for shear thickening suspensions only when the strain amplitude in the frequency sweep was very high ($\gamma > 500\%$). Discrepancies in the use of the modified Cox-Merz rule for shear thickening fluids have been exposed (Chang et al. 2011; Zhang et al. 2008; Fischer et al. 2007; Nguyen et al. 2013; Lee and Wagner 2003). In Fig. 4, we compare steady and oscillatory frequency sweep tests in order to investigate the applicability of the modified Cox-Merz rule. Data of selected concentrations (15, 17.5, 22.5, and 25 wt%) of this study are offered. For all fumed silica concentrations, the best correlation was reached at

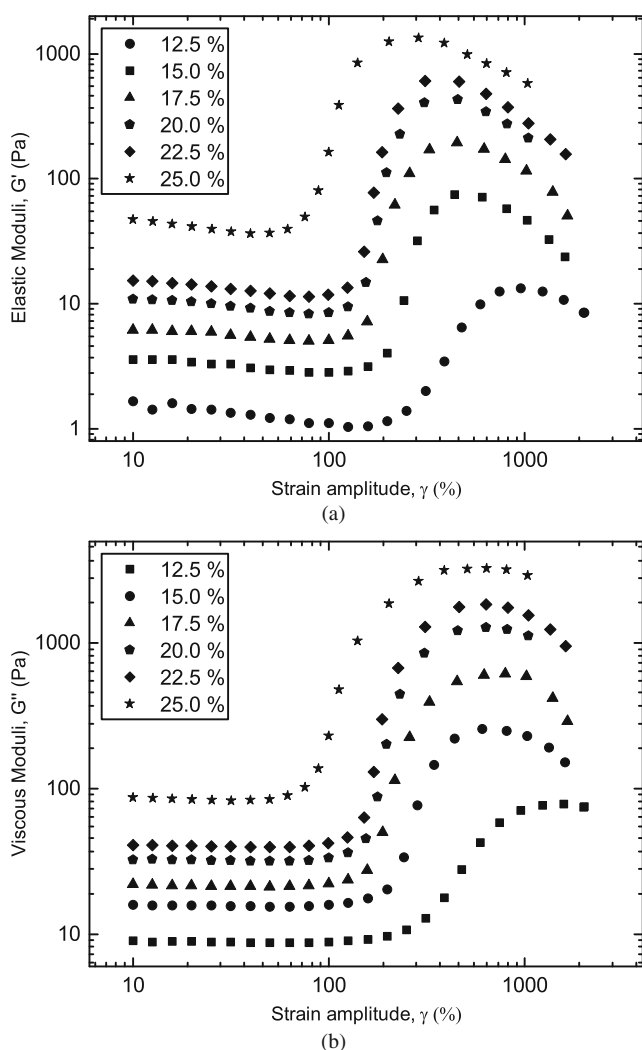
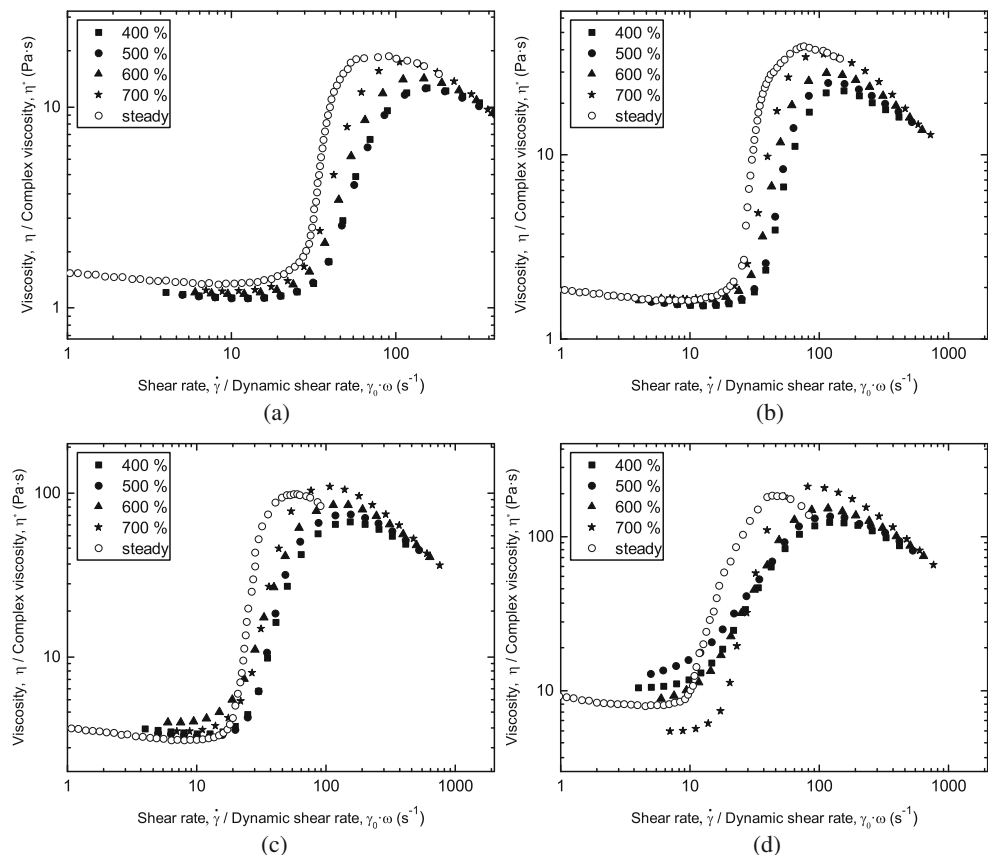


Fig. 3 **a** Elastic moduli (G') and **b** viscous moduli (G'') as a function of strain amplitude of different STF samples with fumed silica concentrations from 12.5 to 25 wt%

Fig. 4 Correlation of steady and oscillatory shear tests using the modified Cox-Merz rule applied to **a** 15 wt%, **b** 17.5 wt%, **c** 22.5 wt%, and **d** 25 wt% fumed silica-polypropylene glycol (PPG) suspensions. The data comes from oscillatory frequency sweeps for $1 < \omega < 100 \text{ rad}\cdot\text{s}^{-1}$ at four different strains (from 400 to 700%) and steady shear rates reproduced from Fig. 1



high strain amplitude (700%) which is applied in the region of shear thinning although the superposition in the shear thickening transition was poor. The results obtained with the other studied strain amplitudes tests were even more poorly superpositioned in the region of shear thickening but were still acceptable at the shear thinning region. The different regimes and transitions were obtained from the evolution of the slopes like we also performed in steady shear test. This is consistent with the results obtained by Lee and Wagner (2003). On the other hand, Fischer et al. (2007) found a poor correlation of the pre-transition regime but a similar correlation for the shear thickening regime. Modified Cox-Merz rule not only has been controversial in shear thickening fluids but also in other non-Newtonian fluids. Yang et al. (2006) studied a similar correlation for MR shear thinning fluids obtaining positive fitting results. However, the fluids tested in their investigation did not show nonlinear behavior as we obtained in our study (Fig. 1)

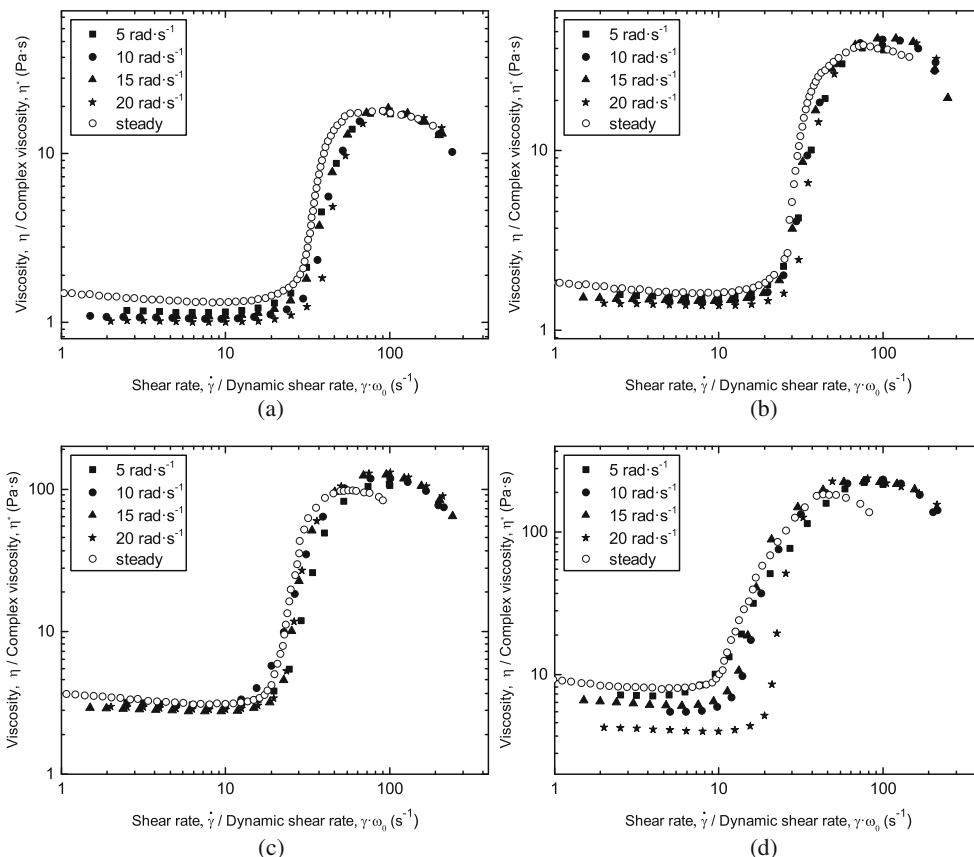
Galindo-Rosales et al. (2009) introduced a modification in the comparison of steady and oscillatory data in STF, but this correlation was never used nor demonstrated any further in the bibliography. They represented the complex viscosity obtained from strain sweep at a fixed frequency:

$$\eta^*(\gamma \cdot \omega_0) = \eta(\dot{\gamma}) \quad (2)$$

They found a qualitative match of this oscillatory shear rate with steady shear, although it was only tested for one type of suspension (10.378 wt% R816 in PPG400) and only one test at $1 \text{ rad}\cdot\text{s}^{-1}$ was performed.

In Fig. 5, we present the comparison of oscillatory strain sweeps at different fixed frequencies for different fumed silica concentrations. We have found in these results a much better correlation between steady and oscillatory results. In the four concentrations illustrated, it can be seen how this method is best correlated at low concentrations and with a frequency sweep test of $5 \text{ rad}\cdot\text{s}^{-1}$. In order to quantify the improvement of the proposed method, we compared the errors of the best correlation between steady and oscillatory shear using the modified Cox-Merz rule (which was reached with oscillatory frequency sweeps at $\gamma = 700\%$) and the best correlation obtained with the proposed method (which was reached oscillatory strain sweeps at $\omega = 5 \text{ rad}\cdot\text{s}^{-1}$). In this case, we have obtained a mean improvement of 34.9% in the correlation error value. This percentage was achieved from the mean value of all STF samples with different weight fractions studied in this investigation. At the same time, it is possible to observe how the poorest correlation using the proposed method was produced at the highest concentration of 25 wt%, although correlation values at $5 \text{ rad}\cdot\text{s}^{-1}$ were still acceptable (improvement of 15.2% in the correlation

Fig. 5 Correlation of steady and oscillatory shear using strain sweep tests at fixed frequencies with **a** 15 wt%, **b** 17.5 wt%, **c** 22.5 wt%, and **d** 25 wt% fumed silica-PPG suspensions. The data comes from oscillatory strain sweeps for $10 < \gamma < 2000\%$ at four different frequencies (from 5 to 20 $\text{rad}\cdot\text{s}^{-1}$) and steady shear rates reproduced from Fig. 1



error value when it is compared with the same fumed silica concentration using the modified Cox-Merz rule). In all concentrations, the poorest correlation regime was obtained in the post-transition state.

Furthermore, we have noticed in both methods (modified Cox-Merz rule and the proposed method) that the correlation get worse as fumed silica concentration is increased. We have attributed this response to the dramatic discontinuous jump of the viscosity at high concentrations. However, the improvement in the global correlation obtained for all STF regimes is positively valuable. The significance of this correlation is the prediction of steady or oscillatory behavior from the data obtained in the oscillatory or steady shear tests, respectively, for instance in circumstances in which one of them is not feasible or is difficult to measure.

Based on the principle of stress-controlled phenomenon attributed to shear thickening colloidal suspensions (Fischer et al. 2007; Bender and Wagner 1996), Lee and Wagner (2003) developed an equation which states that during oscillation tests, shear thickening onset occurs when $\tau \geq \tau_c$, so the critical strain required is calculated from:

$$\gamma_c \approx \frac{\tau_c}{\eta_c \cdot \omega} \tag{3}$$

where η_c is the shear viscosity at the onset of shear thickening and τ_c is the critical stress, both

determined from the steady shear tests. Based on Eq. (3), we obtained Fig. 6 where the experimental points of the critical strain as functions of frequency (from both oscillatory frequency and strain sweeps) are plotted. Furthermore, the lines are obtained from the steady shear results of the Fig. 1. For all concentrations studied, the oscillatory data follow the same trend as lines of data from steady shear.

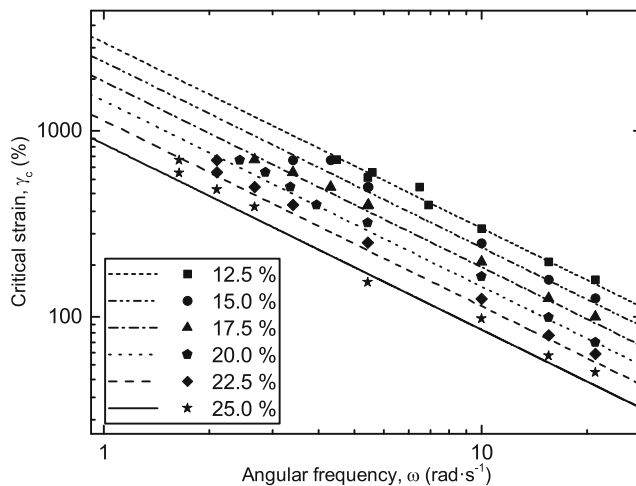


Fig. 6 Critical strain as a function of frequency for different STF samples with fumed silica concentrations from 12.5 to 25 wt%

The maximum error in the fit (17.6%) was found in the concentration of 25 wt%. In the results, we can observe how the critical strain for shear thickening decreases with an increase in frequency. Moreover, the critical strain increases with increasing weight fraction; this relationship is consistent with the results of steady shear. Previously, wall slip influence over high amplitudes and frequencies results has been reported (Chang et al. 2011; Fischer et al. 2007). The variation of critical strain as a function of frequency in high-frequency cases is an apparent plateau (Lee and Wagner 2003). This effect has not been observed in the samples studied in this work.

Conclusions

In this study, we performed a complete rheological characterization of fumed silica suspensions at different weight fractions in polypropylene glycol under both steady and oscillatory shear experiments. The following conclusions have been obtained:

1. Under steady flow, both the critical and maximum viscosity are strongly dependent on the fumed silica weight fraction; moreover, values of shear stress when this happened are also highly dependent. It is essential to recognize the response of STFs in order to progress in the development and design of new applications based on STFs. For that reason, all those properties have been analyzed and quantified to develop and design STUs based on these novel fluids. The applications of this device will be investigated in the automotive field for use in energy-absorbing mechanisms in the case of rollover.
2. Under oscillatory flow, the modified Cox-Merz rule does not offer a good approach to steady shear experiments. However, the use of oscillatory strain sweep tests has enhanced the correlation in all STFs regimes and it has offered an improvement of 34.9% in the correlations in comparison to the modified Cox-Merz rule. These results bring new direction to the research of the correlation between steady and oscillatory shear tests.

Acknowledgments We thank IMDEA Materials Institute for providing us with facilities.

Funding information This research was supported by the Ministerio de Economía y Competitividad, Spain, under grant TRA2014-56471-C4-1-R.

References

Barnes HA (1989) Shear-thickening (Dilatancy) in suspensions of nonaggregating solid particles dispersed in Newtonian liquids. *J Rheol* 33(2):329–366. <https://doi.org/10.1122/1.550017>

- Bender J, Wagner NJ (1996) Reversible shear thickening in monodisperse and bidisperse colloidal dispersions. *J Rheol* 40(5):899–916. <https://doi.org/10.1122/1.550767>
- Bossis G, Brady JF (1989) The rheology of Brownian suspensions. *J Chem Phys* 91(3):1866–1874. <https://doi.org/10.1063/1.457091>
- Brown E, Jaeger HM (2012) The role of dilation and confining stresses in shear thickening of dense suspensions. *J Rheol* 56(5):875–923. <https://doi.org/10.1122/1.4709423>
- Brown E, Jaeger HM (2014) Shear thickening in concentrated suspensions: phenomenology, mechanisms and relations to jamming. *Rep Prog Phys* 77(4):046602. <https://doi.org/10.1088/0034-4885/77/4/046602>
- Brown E, Zhang H, Forman NA, Maynor BW, Betts DE, DeSimone JM, Jaeger HM (2010) Shear thickening in densely packed suspensions of spheres and rods confined to few layers. *J Rheol* 54(5):1023–1046. <https://doi.org/10.1122/1.3474580>
- Brown E, Forman NA, Orellana CS, Zhang H, Maynor BW, Betts DE, DeSimone JM, Jaeger HM (2010) Generality of shear thickening in dense suspensions. *Nat Mater* 9(3):220. <https://doi.org/10.1038/nmat2627>
- Chang L, Friedrich K, Schlarb AK, Tanner R, Ye L (2011) Shear-thickening behaviour of concentrated polymer dispersions under steady and oscillatory shear. *J Mater Sci* 46(2):339–346. <https://doi.org/10.1007/s10853-010-4817-5>
- Cheng X, McCoy JH, Israelachvili JN, Cohen I (2011) Imaging the microscopic structure of shear thinning and thickening colloidal suspensions. *Science* 333(6047):1276–1279. <https://doi.org/10.1126/science.1207032>
- Ding J, Tracey P, Li W, Peng G, Whitten PG, Wallace GG (2013) Review on shear thickening fluids and applications. *Textiles and Light Industrial Science and Technology* 2(4):161–173
- Doraiswamy D, Mujumdar AN, Tsao I, Beris AN, Danforth SC, Metzner AB (1991) The Cox-Merz rule extended: a rheological model for concentrated suspensions and other materials with a yield stress. *J Rheol* 35(4):647–685. <https://doi.org/10.1122/1.550184>
- Egres RG, Wagner NJ (2005) The rheology and microstructure of acicular precipitated calcium carbonate colloidal suspensions through the shear thickening transition. *J Rheol* 49(3):719–746. <https://doi.org/10.1122/1.1895800>
- Egres RG, Nettesheim F, Wagner NJ (2006) Rheo-SANS investigation of acicular-precipitated calcium carbonate colloidal suspensions through the shear thickening transition. *J Rheol* 50(5):685–709. <https://doi.org/10.1122/1.2213245>
- Fischer C, Plummer CJG, Michaud V, Bourban PE, Manson JAE (2007) Pre- and post-transition behavior of shear-thickening fluids in oscillating shear. *Rheol Acta* 46(8):1099–1108. <https://doi.org/10.1007/s00397-007-0202-y>
- Galindo-Rosales FJ (2016) Complex fluids in energy dissipating systems. *Appl Sci* 6(8):206. <https://doi.org/10.3390/app6080206>
- Galindo-Rosales FJ, Rubio-Hernández F, Velázquez-Navarro JF (2009) Shear-thickening behavior of Aerosil®r816 nanoparticles suspensions in polar organic liquids. *Rheol Acta* 48(6):699–708. <https://doi.org/10.1007/s00397-009-0367-7>
- Galindo-Rosales FJ, Rubio-Hernández FJ, Sevilla A (2011a) An apparent viscosity function for shear thickening fluids. *J Non-Newtonian Fluid Mech* 166(5-6):321–325. <https://doi.org/10.1016/j.jnnfm.2011.01.001>
- Galindo-Rosales FJ, Rubio-Hernández FJ, Sevilla A, Ewoldt RH (2011b) How Dr. Malcom M. Cross may have tackled the development of ‘An apparent viscosity function for shear thickening fluids’. *J Non-Newtonian Fluid Mech* 166(23-24):1421–1424. <https://doi.org/10.1016/j.jnnfm.2011.08.008>
- Galvez P, Quesada A, Martínez MA, Abenojar J, Boada MJL, Diaz V (2017) Study of the behaviour of adhesive joints of steel with

- CFRP for its application in bus structures. *Compos Part B-Eng* 129:41–46. <https://doi.org/10.1016/j.compositesb.2017.07.018>
- García-Rojas B, Bautista F, Puig JE, Manero O (2009) Thermodynamic approach to rheology of complex fluids: Flow-concentration coupling. *Phys Rev E* 80(3):036313. <https://doi.org/10.1103/PhysRevE.80.036313>
- Gauchía A, Olmeda E, Aparicio F, Díaz V (2011) Bus mathematical model of acceleration threshold limit estimation in lateral rollover test. *Veh Syst Dyn* 49(10):1695–1707. <https://doi.org/10.1080/00423114.2010.544745>
- Gürgen S, Kuşhan MC, Li W (2016) The effect of carbide particle additives on rheology of shear thickening fluids. *Korea-Aust Rheol J* 28(2):121–128. <https://doi.org/10.1007/s13367-016-0011-x>
- Gürgen S, Li W, Kuşhan MC (2016) The rheology of shear thickening fluids with various ceramic particle additives. *Mater Des* 104:312–319. <https://doi.org/10.1016/j.matdes.2016.05.055>
- He Q, Gong X, Xuan S, Jiang W, Chen Q (2015) Shear thickening of suspensions of porous silica nanoparticles. *J Mater Sci* 50(18):6041–6049. <https://doi.org/10.1007/s10853-015-9151-5>
- Hoffman RL (1972) Discontinuous and dilatant viscosity behavior in concentrated suspensions. I. Observation of a flow instability. *Trans Soc Rheol* 16(1):155–173. <https://doi.org/10.1122/1.549250>
- Hoffman RL (1974) Discontinuous and dilatant viscosity behavior in concentrated suspensions. II. Theory and experimental tests. *J Colloid Interface Sci* 46(3):491–506. [https://doi.org/10.1016/0021-9797\(74\)90059-9](https://doi.org/10.1016/0021-9797(74)90059-9)
- Khandavalli S, Rothstein JP (2015) Large amplitude oscillatory shear rheology of three different shear-thickening particle dispersions. *Rheol Acta* 54(7):601–618. <https://doi.org/10.1007/s00397-015-0855-x>
- Khandavalli S, Rothstein JP (2014) Extensional rheology of shear-thickening fumed silica nanoparticles dispersed in an aqueous polyethylene oxide solution. *J Rheol* 58(2):411–431. <https://doi.org/10.1122/1.4864620>
- Laha A, Majumdar A (2016) Interactive effects of p-aramid fabric structure and shear thickening fluid on impact resistance performance of soft armor materials. *Mater Des* 89:286–293. <https://doi.org/10.1016/j.matdes.2015.09.077>
- Lee YS, Wagner NJ (2003) Dynamic properties of shear thickening colloidal suspensions. *Rheol Acta* 42(3):199–208. <https://doi.org/10.1007/s00397-002-0290-7>
- Lee YS, Wagner NJ (2006) Rheological properties and small-angle neutron scattering of a shear thickening, nanoparticle dispersion at high shear rates. *Ind Eng Chem Res* 45(21):7015–7024. <https://doi.org/10.1021/ie0512690>
- Li W, Xiong D, Zhao X, Sun L, Liu J (2016) Dynamic stab resistance of ultra-high molecular weight polyethylene fabric impregnated with shear thickening fluid. *Mater Des* 102:162–167. <https://doi.org/10.1016/j.matdes.2016.04.006>
- Liang CC, Le GN (2009) Bus rollover crashworthiness under european standard: an optimal analysis of superstructure strength using successive response surface method. *Int J Crashworthiness* 14(6):623–639. <https://doi.org/10.1080/13588260902920670>
- Lin NYC, Guy BM, Hermes M, Ness C, Sun J, Poon WCK, Cohen I (2015) Hydrodynamic and contact contributions to continuous shear thickening in colloidal suspensions. *Phys Rev Lett* 115(22):228304. <https://doi.org/10.1103/PhysRevLett.115.228304>
- Majumdar A, Butola BS, Srivastava A (2014) Development of soft composite materials with improved impact resistance using Kevlar fabric and nano-silica based shear thickening fluid. *Mater Des* 54:295–300. <https://doi.org/10.1016/j.matdes.2013.07.086>
- Manero O, Pérez-López JH, Escalante JI, Puig JE, Bautista F (2007) A thermodynamic approach to rheology of complex fluids: The generalized BMP model. *J Non-Newtonian Fluid Mech* 146(1–3):22–29. <https://doi.org/10.1016/j.jnnfm.2007.02.012>
- Maranzano BJ, Wagner NJ (2002) Flow-small angle neutron scattering measurements of colloidal dispersion microstructure evolution through the shear thickening transition. *J Chem Phys* 117(22):10291–10302. <https://doi.org/10.1063/1.1519253>
- Mari R, Seto R, Morris JF, Denn MM (2014) Shear thickening, frictionless and frictional rheologies in non-Brownian suspensions. *J Rheol*, 58(6). <https://doi.org/10.1122/1.4890747>
- Mewis J, Wagner NJ (2012) *Colloidal suspension rheology*. Cambridge University Press, Cambridge
- Nguyen HV, Andreassen E, Kristiansen H, Johannessen R, Hoivik N, Aasmundtveit KE (2013) Rheological characterization of a novel isotropic conductive adhesive – epoxy filled with metal-coated polymer spheres. *Mater Des* 46:784–793. <https://doi.org/10.1016/j.matdes.2012.11.036>
- Park SJ, Yoo WS (2008) Rollover analysis for the body section structure of a large bus using beam and non-linear spring elements. *Proc Inst Mech Eng D J Automob Eng* 222(6):955–962. <https://doi.org/10.1243/09544070JAUTO474>
- Raghavan SR, Khan SA (1997) Shear-thickening response of fumed silica suspensions under steady and oscillatory shear. *J Colloid Interface Sci* 185(1):57–67. <https://doi.org/10.1006/jcis.1996.4581>
- Seto R, Mari R, Morris JF, Denn MM (2013) Discontinuous shear thickening of frictional hard-sphere suspensions. *Phys Rev Lett*, 111(21). <https://doi.org/10.1103/PhysRevLett.111.218301>
- Tian T, Nakano M (2017) Design and testing of a rotational brake with shear thickening fluids. *Smart Mater Struct* 26(3):035038. <https://doi.org/10.1088/1361-665X/aa5a2c>
- Tian T, Peng G, Li W, Ding J, Nakano M (2015) Experimental and modelling study of the effect of temperature on shear thickening fluids. *Korea-Aust Rheol J* 27(1):17–24. <https://doi.org/10.1007/s13367-015-0003-2>
- Turcio M, Chávez AE, López-Aguilar J, Vargas RO, Capella A, Manero O (2018) Dissipative structures in shear-thickening complex fluids. *Phys Fluids* 30(11):114104. <https://doi.org/10.1063/1.5051768>
- Vázquez-Quesada A, Wagner NJ, Ellero M (2017) Planar channel flow of a discontinuous shear-thickening model fluid: Theory and simulation. *Phys Fluids* 29(10):103104. <https://doi.org/10.1063/1.4997053>
- Wagner NJ, Brady JF (2009) Shear thickening in colloidal dispersions. *Phys Today* 62(10):27–32
- Yang YB, Chen G, Li L, Li WH (2006) On the extended Rutgers–Delaware rule for mr suspensions under magnetic fields. *Int J Mod Phys B* 20(05):579–592. <https://doi.org/10.1142/S0217979206033449>
- Zhang G, Wu J, Tang L, Li J, Lai G, Zhong M (2014) Rheological behaviors of fumed silica/low molecular weight hydroxyl silicone oil. *J Appl Polym Sci* 131(17):n/a. <https://doi.org/10.1002/app.40722>
- Zhang SS, Zhang YJ, Wang HW (2010) Effect of particle size distributions on the rheology of Sn/Ag/Cu lead-free solder pastes. *Mater Des* 31(1):594–598. <https://doi.org/10.1016/j.matdes.2009.07.001>
- Zhang XZ, Li WH, Gong XL (2008) The rheology of shear thickening fluid (STF) and the dynamic performance of an STF-filled damper. *Smart Mater Struct* 17(3):035027. <https://doi.org/10.1088/0964-1726/17/3/035027>